

Preparation of Optoelectronic Devices Based on AlN/AlGa_N Superlattices

M. Holtz,^{a,b} G. Kipshidze,^c A. Chandolu,^c J. Yun,^c B. Borisov,^c V. Kuryatkov,^c K. Zhu,^c
S. N. G. Chu,^d S. A. Nikishin,^{b,c} and H. Temkin^{b,c}

^a Department of Physics, ^b Nano Tech Center, ^c and Department of Electrical Engineering
Texas Tech University, Lubbock, Texas 79409

^d Agere Systems, Murray Hill, NJ 07974

ABSTRACT

We present results on growth and fabrication experiments of AlN/AlGa_N superlattices for ultraviolet (UV) optoelectronic devices. Superlattices with extremely short periods have been studied. The AlN “barrier” layers are 0.5 nm thick, and the Al_xGa_{1-x}N “wells” are 1.25 nm thick, with $x \sim 0.08$. This combination gives an average AlN mole fraction of 0.63 across one full period. The superlattice periods, AlN mole fractions, and energy gaps are determined using TEM, X-ray diffraction, and optical reflectance. They are all consistent with each other. For device fabrication, p-i-n structures are grown doped with Si (n-type) and Mg (p-type). The acceptor activation energy of ~ 0.2 eV is found. Mesa structures are plasma etched using chlorine chemistry. Etch rates of AlN are $\sim 1/3$ those of GaN under identical circumstances. Etch rates of 250 nm/min are used for the device structures. A light emitting diode, with primary emission at 280 nm is reported, and a detector with sensitivity edge at 260 nm are reported.

INTRODUCTION

There is currently considerable interest in making optoelectronic devices operating in the ultraviolet (UV). Light emitting diodes (LEDs) with emission wavelengths between 340 nm and 280 nm are potentially useful for a number of important applications, from fluorescence excitation to data storage. High performance UV photodetectors having responsivity below ~ 280 nm would be highly useful because they would not respond to the visible solar spectrum, i.e., they would be solar-blind. The most promising material for achieving high performance at short wavelength is the Al_xGa_{1-x}N alloy system [1-5], which can be grown epitaxially in the wurtzite structure across the full composition range [6].

There are important problems associated with growing Al_xGa_{1-x}N. First, substrates used for the epitaxial growth (sapphire, silicon, and silicon carbide) each induces stress in the layers due to a combination of lattice mismatch and thermal stress [7,8]. Second, to achieve a band gap above 4.4 eV (below 280 nm), a composition of $x > 0.5$ is needed. While it is possible to dope these alloys n-type (Si), producing p-type (Mg) material with high hole concentrations is inherently difficult because the acceptor level grows deeper with higher Al content.

Our recent work has shown that diodes based on superlattices (SLs) of AlN/AlGaInN can be used to produce both LEDs with light emission down to 280 nm [5] and photodetectors with sensitivity edge near 260 nm [9]. This is accomplished using SLs of AlN and AlGaInN with extremely small well and barrier thicknesses. The average AlN mole fraction is very high in these structures, over 0.6, providing the necessary large optical gap, and the wells are heavily doped to produce a high average carrier concentration.

Report Documentation Page			Form Approved OMB No. 0704-0188		
Public reporting burden for the collection of information is estimated to average 1 hour per response, including the time for reviewing instructions, searching existing data sources, gathering and maintaining the data needed, and completing and reviewing the collection of information. Send comments regarding this burden estimate or any other aspect of this collection of information, including suggestions for reducing this burden, to Washington Headquarters Services, Directorate for Information Operations and Reports, 1215 Jefferson Davis Highway, Suite 1204, Arlington VA 22202-4302. Respondents should be aware that notwithstanding any other provision of law, no person shall be subject to a penalty for failing to comply with a collection of information if it does not display a currently valid OMB control number.					
1. REPORT DATE 2002		2. REPORT TYPE		3. DATES COVERED 00-00-2002 to 00-00-2002	
4. TITLE AND SUBTITLE Preparation of Optoelectronic Devices Based on AlN/AlGa_N Superlattices			5a. CONTRACT NUMBER		
			5b. GRANT NUMBER		
			5c. PROGRAM ELEMENT NUMBER		
6. AUTHOR(S)			5d. PROJECT NUMBER		
			5e. TASK NUMBER		
			5f. WORK UNIT NUMBER		
7. PERFORMING ORGANIZATION NAME(S) AND ADDRESS(ES) Texas Tech University,2500 Broadway,Lubbock ,TX,79409			8. PERFORMING ORGANIZATION REPORT NUMBER		
9. SPONSORING/MONITORING AGENCY NAME(S) AND ADDRESS(ES)			10. SPONSOR/MONITOR'S ACRONYM(S)		
			11. SPONSOR/MONITOR'S REPORT NUMBER(S)		
12. DISTRIBUTION/AVAILABILITY STATEMENT Approved for public release; distribution unlimited					
13. SUPPLEMENTARY NOTES					
14. ABSTRACT We present results on growth and fabrication experiments of AlN/AlGa_N superlattices for ultraviolet (UV) optoelectronic devices. Superlattices with extremely short periods have been studied. The AlN ?barrier? layers are 0.5 nm thick, and the Al_xGa_{1-x}N ?wells? are 1.25 nm thick, with x ~ 0.08. This combination gives an average AlN mole fraction of 0.63 across one full period. The superlattice periods, AlN mole fractions, and energy gaps are determined using TEM, X-ray diffraction, and optical reflectance. They are all consistent with each other. For device fabrication, p-i-n structures are grown doped with Si (n-type) and Mg (p-type). The acceptor activation energy of ~ 0.2 eV is found. Mesa structures are plasma etched using chlorine chemistry. Etch rates of AlN are ~ 1/3 those of GaN under identical circumstances. Etch rates of 250 nm/min are used for the device structures. A light emitting diode, with primary emission at 280 nm is reported, and a detector with sensitivity edge at 260 nm are reported.					
15. SUBJECT TERMS					
16. SECURITY CLASSIFICATION OF:			17. LIMITATION OF ABSTRACT Same as Report (SAR)	18. NUMBER OF PAGES 6	19a. NAME OF RESPONSIBLE PERSON
a. REPORT unclassified	b. ABSTRACT unclassified	c. THIS PAGE unclassified			

GROWTH OF AlN/AlGaN SUPERLATTICES

Device material was grown on sapphire substrates using gas source molecular beam epitaxy with ammonia as the nitrogen source [10]. The growth started with a 40-nm thick layer of AlN followed by a 1- μm thick buffer layer of GaN. This GaN layer reduces the dislocation density in the device SL. Dislocation density in the top part of the GaN layer was estimated from TEM measurements at $\sim 6 \times 10^9 \text{ cm}^{-2}$. The SL-based device structures, having a total thickness of $\sim 0.7 \mu\text{m}$ (330 total periods), were grown over the GaN layer.

For the LEDs, AlN barriers were 1.25 nm (5 monolayers) thick and the $\text{Al}_x\text{Ga}_{1-x}(\text{In})\text{N}$ wells, with x from 0.06 to 0.08, were 0.5 and 0.75 nm (2–3 monolayers) thick in both p- and n-type SLs. In the active region of the device, consisting of five undoped barrier/well pairs and placed between n- and p-regions, the well thickness was increased to 0.75 nm to increase the electroluminescence efficiency [5]. These thicknesses are below the critical layer thickness [11]. No additional dislocations were observed in the SL structure by transmission electron microscopy (TEM) [10].

For the photodetectors, two n- and p-type AlN/AlGa(In)N superlattices were grown successively followed by a 10-nm $\text{Al}_{0.08}\text{Ga}_{0.092}(\text{In})\text{N}:\text{Mg}$ contact layer. Each n- and p-type SL consisted of 150 pairs of $\text{Al}_{0.08}\text{Ga}_{0.92}(\text{In})\text{N}$ quantum wells, 0.5 nm thick, separated by ~ 1.0 nm barriers of AlN. Because of the high growth temperature $\sim 800^\circ\text{C}$, the InN content in the wells was low, approximately 10^{17} cm^{-3} , as shown by secondary ion mass spectrometry measurements.

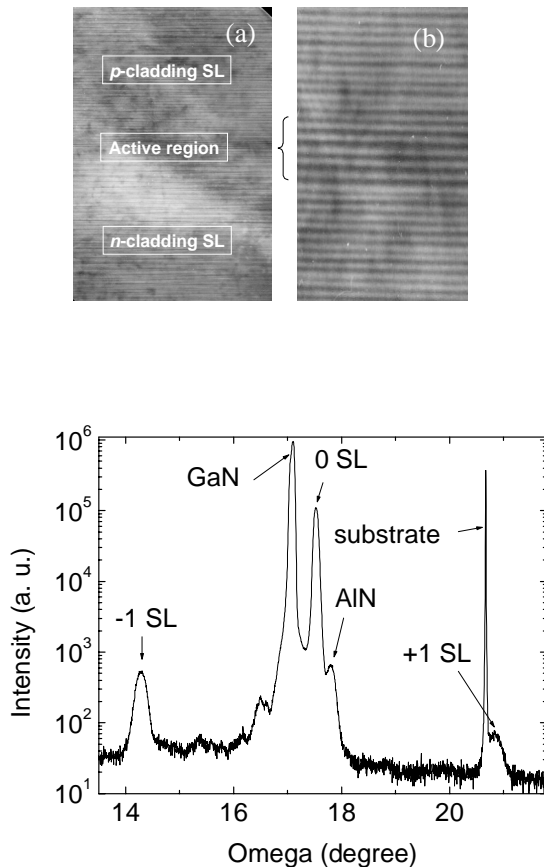


Fig. 2 X-ray diffraction of a SL.

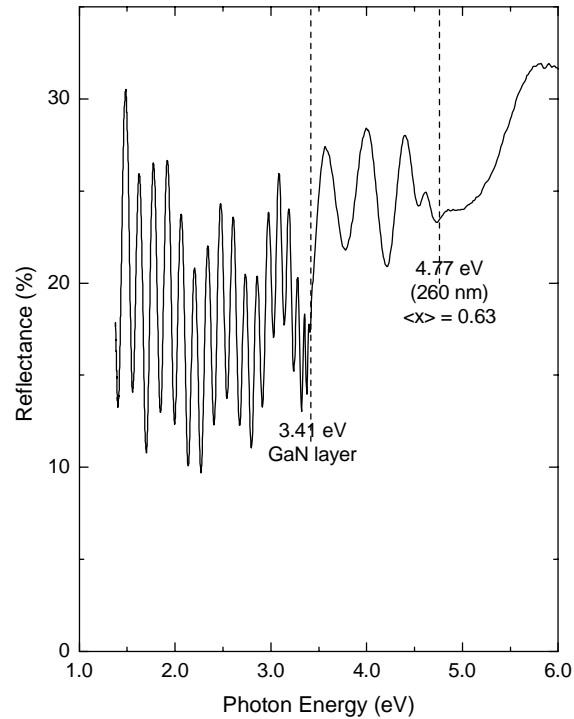


Fig. 3 Reflectance spectrum (and derivative) showing the SL optical gap (4.66 eV).

Figure 1 shows a TEM cross-section of one SL, exhibiting well defined layers with abrupt interfaces. The average thickness determined from TEM data is in good agreement with estimates based on growth calibrations and results of X-ray diffraction measurements, as shown in Fig. 2. The average composition in our SL structures is estimated to be $x = 0.63$ from the X-ray. This is verified by reflectance measurements in Fig. 3 which show that the optical gap is determined by the *average* SL composition. This is reasonable, since our well layers are too thin for confinement effects. Temperature dependent I-V measurements show the hole activation energy to be 207 ± 10 meV [12], consistent with our activation energy measured for thick epitaxial layer of alloys having the same composition [13]. Hole concentrations were $(0.7 - 1.1) \times 10^{18} \text{ cm}^{-3}$. We thus demonstrate short wavelength and high p-type carrier concentrations.

PLASMA PROCESSING

Mesa structures are plasma etched with diameters ranging from 120 to 400 μm . A commercial system is used for etching with Cl_2/Ar gas mixture. Samples are mounted on 200 mm silicon wafers coated on the processing side by SiO_2 . The baseline pressure of the etching system is 2×10^{-6} Torr. The gases are injected through a showerhead located approximately 100 mm above the sample. A high-density inductively-coupled plasma (ICP) discharge is generated by applying 13.56 MHz rf power. The wafer electrode is powered separately by a 600 W (maximum) generator operated at 13.56 MHz for reactive ion etching (RIE). During the etching process, the substrate is cooled by He gas flowing from the electrostatic chuck, with no temperature control. We estimate the wafer temperature to remain below $\sim 100^\circ\text{C}$ during our experiments. Etch depths are determined using a stylus profilometer. A scanning electron microscope (SEM) and an atomic force microscope (AFM) were used to determine etch anisotropy and surface properties.

AFM measurements of the as-grown nitride layers reveal RMS surface roughness to be 4 – 5 nm. Because little is known about the etch properties of AlN, we conducted studies to determine etch rate and induced roughness. Figure 4 shows etch rate of GaN and AlN vs. ICP power. During these runs, the RIE power, chamber pressure, and Cl_2/Ar gas flow rate were kept at 150 W, 8 mTorr, and 20/5 sccm, respectively. The GaN etch rate rises from 300 to 630

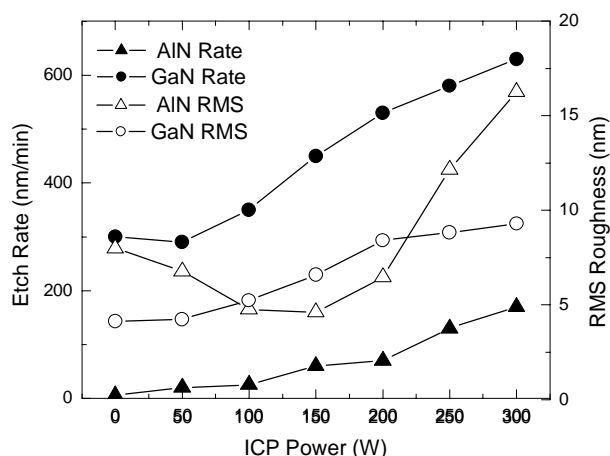


Fig. 4 Etch rate (filled) and RMS roughness (open) vs. ICP power for GaN and AlN.

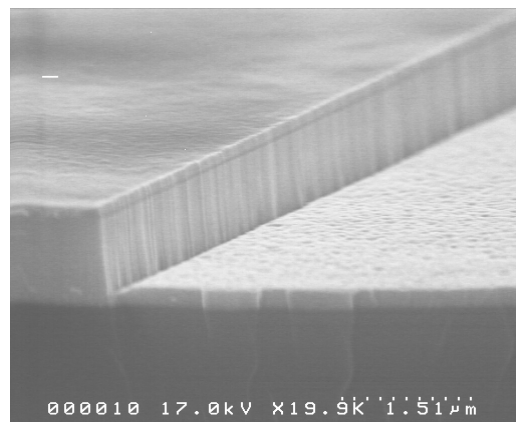


Fig. 5 SEM showing typical anisotropy of etched devices.

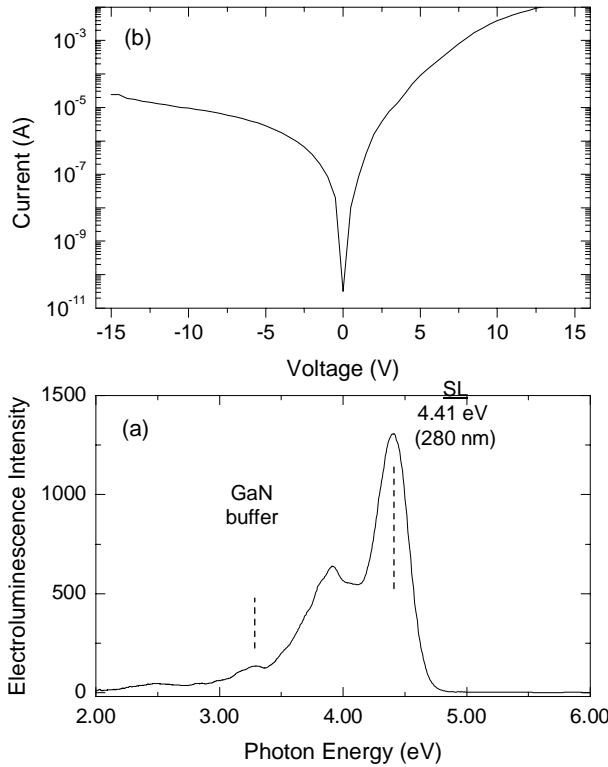


Fig. 6 (a) Electroluminescence spectrum of LED showing 4.41 eV emission.
(b) Room temperature I-V characteristics.

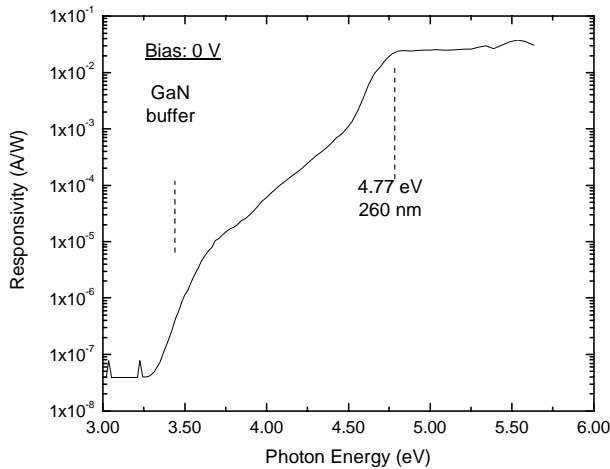


Fig. 7 AlN/AlGa(In)N photodiode spectral responsivity measured at zero bias under front illumination.

nm/min and the RMS roughness accordingly increased from 4 nm to 9 nm. AlN etches at a rate of 5 nm/min, at zero ICP power, gradually rising to 170 nm/min at 300 W. Over this same range, the roughness also has an increasing trend. Increased ICP power produces more reactive ions and neutrals, which in turn elevates the etch rate [14-16]. The measurements imply that surface roughness is correlated to etch rate, a correlation observed in studies varying the other etch parameters RIE power, Cl_2/Ar flow ratio, and chamber pressure. Figure 4 shows that the etch rate of GaN is ~ 3 times that of AlN due to the higher bond energy of the latter. In contrast to the lower etch rate of AlN, the RMS roughness is higher than GaN. It should be noted that the as-grown AlN had a slightly higher roughness than that of GaN, 6.3 nm compared to 4.5 nm. These studies are used to select etching conditions for our mesa devices which do not produce excessive roughness, while providing an acceptable etch rate ~ 100 nm/min and etching isotropically [17]. We used ICP power of 300 W, RIE power of 150 W, chamber pressure of 8 mTorr, and 20/5 sccm flow rate ratio (Cl_2/Ar). A SEM cross-section of etched AlN is shown in Fig. 5, verifying that our conditions produce a highly anisotropic etch with vertical sidewalls.

DEVICE RESULTS

In Fig. 6 we show typical electro-luminescence (a) and I-V curves (b) from LEDs fabricated using these methods. Mesa diameters range from 120 to 400 μm . Turn-on voltages range between 3.5 and 4.0 V, and series resistances are approximately 90 Ω . The zero forward bias current is ~ 20 pA and

leakage currents of 20 – 30 μA are found under reverse voltages of 15 V. The low leakage currents are consistent with high quality of etched mesa sidewalls. The devices were able to withstand dc current densities of 500 A/cm^2 at room temperature. Figure 6a shows the electroluminescence spectrum for this device, which exhibits the shortest emission wavelength that we are aware of. The dominant band is at 4.41 eV (280 nm), with defect-related emission at ~ 3.91 eV and GaN buffer layer emission at ~ 3.35 eV.

Measurements of the spectral responsivity were done at zero bias using a mercury lamp as a light source and a monochromator. Light intensity was measured using a calibrated detector. The responsivity spectrum is shown in Fig. 7. The peak response was obtained at ~ 4.77 eV (260 nm), in excellent agreement with the bandgap of the SLs obtained by reflectivity measurements. Responsivity does not fall off above the bandgap, indicating low surface recombination velocity. Since the carriers are created close to the surface and must diffuse to the junction in order to be collected, this also indicates minority carrier (electron) diffusion length greater than ~ 200 nm, the thickness of the p-type SL. Responsivity decreases below 4.77 eV and it drops off by almost six orders of magnitude at 3.26 eV, showing excellent rejection of visible radiation. The sub-structure visible in the photoresponse in the range of ~ 280 -340 nm is not understood at this time. It may be partially related to absorption in the exposed GaN buffer layer, at the bottom of the device mesa, but this would imply fairly long hole diffusion lengths. Another possibility is the broadening of the absorption edge due to monolayer thickness fluctuations in the well and barrier thickness. We plan to answer some of these questions by growing additional SL structures on AlN buffer layers.

Responsivity of 25 mA/W was measured at wavelength of 260 nm. This corresponds to an external quantum efficiency of 12.5 %. Using the $R_0A \sim 6.2 \times 10^8 \Omega\cdot\text{cm}^2$ determined from current-voltage measurements we calculate the thermal noise limited specific detectivity, at zero-bias, as $D^* = 1.4 \times 10^{12} \text{ cm}\cdot\text{Hz}^{1/2}/\text{W}$.

SUMMARY

Short period SLs of AlN/AlGa(In)N are shown to exhibit large optical energy gap and permit acceptably high hole concentrations in Mg-doped materials. We have experimented with both LEDs and photodetectors using this type of structure. The LEDs show primary emission at 4.41 eV (280 nm). The photodetectors show responsivity maximum at 4.77 eV (260 nm), which then drops by five orders of magnitude by 3.26 eV.

ACKNOWLEDGMENTS

The authors acknowledge support from the NSF (ECS-0070240 and ECS-9871290), DARPA (Dr. J. Carrano), U. S. Army SBCCOM, NATO Science for Peace (974505), and the J. F. Maddox Foundation.

REFERENCES

1. K. Tadamoto, H. Okagawa, Y. Ohuchi, T. Tsunekawa, Y. Imada, H. Kato, and T. Taguchi, *Jpn.J.Appl.Phys.* **40**, L583 (2001).
2. T. Nishida, H. Saito, and N. Kobayashi, *Appl.Phys.Lett.* **78**, 3927 (2001).

3. H. Hirayama, A. Kinoshita, M. Ainoya, A. Hirata, and Y. Aoyagi, *phys.stat.sol.(a)* **188**, 83 (2001).
4. V. Adivarahan, A. Chitnis, J. P. Zhang, M. Shatalov, J. W. Yang, G. Simin, and M. A. Khan, *Appl.Phys.Lett.* **79**, 4240 (2001).
5. G. Kipshidze, V. Kuryatkov, B. Borisov, M. Holtz, S. Nikishin, and H. Temkin, *Appl.Phys.Lett.* **80**, 3682 (2002).
6. M. Holtz, T. Prokofyeva, M. Seon, K. Copeland, J. Vanbuskirk, S. Williams, S. Nikishin, V. Tretyakov, and H. Temkin, *J.Appl.Phys.* **89**, 7977 (2001).
7. M. Holtz, M. Seon, T. Prokofyeva, H. Temkin, R. Singh, F. P. Dabkowski, and T. D. Moustakas, *Appl. Phys. Lett.* **75**, 1757 (1999).
8. T. Prokofyeva, M. Seon, J. Vanbuskirk, M. Holtz, S. A. Nikishin, N. N. Faleev, H. Temkin, and S. Zollner, *Phys. Rev. B* **63**, 125313/1 (2000).
9. V. Kuryatkov, A. Chandolu, B. Borisov, G. Kipshidze, K. Zhu, S. A. Nikishin, H. Temkin, and M. Holtz, *Appl.Phys.Lett.*, (submitted), 2002.
10. G. Kipshidze, V. Kuryatkov, B. Borisov, S. A. Nikishin, M. Holtz, S. N. G. Chu, and H. Temkin, *phys.stat.sol.(a)* **192**, 286 (2002).
11. A. D. Bykhovski, B. L. Gelmont, and M. S. Shur, *J.Appl.Phys.* **78**, 3691 (1995).
12. V. Kuryatkov, K. Zhu, B. Borisov, A. Chandolu, Iu. Gerasoiu, G. Kipshidze, S. N. G. Chu, M. Holtz, Yu. Kudryavtsev, R. Asomoza, S. A. Nikishin, and H. Temkin, *Appl.Phys.Lett.*, (submitted).
13. G. Kipshidze, V. Kuryatkov, B. Borisov, Yu. Kudryatsov, R. Asomoza, S. A. Nikishin, and H. Temkin, *Appl.Phys.Lett.* **80**, 2910 (2002).
14. S. A. Smith, C. A. Wolden, M. D. Bremser, A. D. Hanser, R. F. Davis, and W. V. Lampert, *Appl.Phys.Lett.* **71**, 3631 (1997).
15. S. J. Pearton, J. C. Zolper, R. J. Shul, and F. Ren, *Appl.Phys.Lett.* **86**, 77 (1999).
16. Hyun Cho, C. B. Vartuli, S. M. Donovan, C. R. Abernathy, S. J. Pearton, R. J. Shul, and C. Constantine, *J.Vac.Sci.Technol.A* **16**, 1631 (1998).
17. K. Zhu, V. Kuryatkov, B. Borisov, G. Kipshidze, S. A. Nikishin, H. Temkin, and M. Holtz, *Appl.Phys.Lett.* (in press) 2002.